Context-dependent consequences of lagged effects in demographic models

Eric R. Scott[1], María Uriarte[1], Emilio M. Bruna[1]

[1]Department of Wildlife Ecology and Conservation, University of Florida, Gainesville, Florida 32611-0430 USA
[2]Department of Ecology, Evolution and Environmental Biology, Columbia University 1200 Amsterdam Avenue, New York, New York 10027 USA
[3]Center for Latin American Studies, University of Florida, Gainesville, Florida 32611-5530 USA
[4]Biological Dynamics of Forest Fragments Project, INPA-PDBFF, CP 478, Manaus, Amazonas 69011-970 Brazil

(draft: 8 April 2025)

Abstract

Text of 150 words max summarizing this amazing paper.

Keywords: demography, environmental stochasticity, integral projection models, lagged effects, structured population models, population dynamics

Manuscript elements: Figure~1, figure~2, table~1, appendix~A..

Manuscript type: e-note

Introduction

There is increasing evidence that an organism's current likelihood of growth, survival, or reproduction can be strongly influenced by previous environmental conditions. These *Lagged Effects*, also known as *Delayed Life-history Events* (i.e., DLHEs) (Beckerman et al. 2002), can simultaneously affect an entire cohort (e.g., juveniles hatching during a period of scarcity will all have delayed maturation and lower lifetime fecundity) or only a subset of the population (e.g., cold temperatures in one year lead to reduced flowering by potentially reproductive individuals in the next). In addition, the temporal delay between an environmental event and changes in demographic vital rates depends on both the intensity of the event and its timing relative to the underlying physiological processes (Criley and Lekawatana 1994; Evers et al. 2021). A drought during the early stages of gestation or floral bud formation, for example, might have a much larger impact on the number of fruits or offspring produced than one several months later whose timing coincides with birth or flowering. The delay or intensity of lagged effects can also depend on local ecological conditions, with individuals in some habitats buffered against – or able to recover more quickly from - the delayed effects of environmental variation.

Because Lagged Effects are often directly linked to reproduction and survival, it is thought they could have major consequences for population dynamics (Beckerman et al. 2002). Although there is emerging evidence that this is indeed the case (Williams et al. 2015; e.g., Molowny-Horas et al. 2017; Tenhumberg et al. 2018), broader efforts to test this hypothesis have been hampered by two primary factors: First, detecting lagged effects requires long-term data on both the putative lagged effect (i.e., probability of flowering) and its potential environmental drivers (Metcalf et al. 2015). These coupled data sets are rare (sensu Evers et al. 2021), in part because studies to disentangle lagged effects can be challenging to design and maintain (Kuss et al. 2008). Second, the methods for identifying lagged effects and modeling their demographic impacts can be challenging to implement. Many of the statistical methods have stringent data requirements (Metcalf et al. 2015) and assumptions, while the including complex biological processes in demographic models can render them less tractable. Addressing these obstacles is a major undertaking; the value of doing so will depend on the effort required vs. the potential consequences of failing to consider lagged effects - consequences that range from overestimating projections of population growth rate (i.e., λ) in a conservation setting to drawing invalid conclusions regarding support for the predictions of ecological or evolutionary theory.

Integral Projection Models (i.e., IPMs) are an important and widely used tool for studying demography and population dynamics (Ellner and Rees 2006; Rees and Ellner 2009; Rees et al. 2014). Their flexibility, in concert with a rapidly growing suite of software, data, and other resources (Salguero-Gómez et al. 2015; Ellner et al. 2016; Levin et al. 2021), have facilitated their use to study a wide range of topics in ecology, evolution, and conservation Crone et al. (2011). Mathematical and statistical advances (e.g., Williams et al. 2012; Brooks et al. 2019) have rapidly expand the scope of questions and biological processes that can be investigated with these models (e.g., Metcalf et al. 2015; Ellner et al. 2016; Rees and Ellner 2016). Here we investigate how including lagged effects in Integral Projection

Models influences projections of λ and population structure.

We have previously shown that the effects of precipitation extremes on the demographic vital rates of an Amazonian understory herb (*Heliconia acuminata*, Heliconiaceae) can be delayed up to 36 months (Scott et al. 2022), with the presence and duration of these lagged effects varying by vital rate and habitat. We parameterized three classes of Integral Projection Models - a deterministic IPM, a stochastic IPM, and a stochastic IPM with lagged effects of precipitation on vital rates - for populations in two habitat type (i.e., continuous forest vs. forest fragments). Based on previous studies (Bruna et al. 2002; Bruna and Kress 2002; Bruna 2003; Bruna and Oli 2005) and demographic theory (Tuljapurkar 1990; Caswell 2001) we predicted that:

(i) projections of λ would be lower in forest fragments than in continuous forest for all model types,
(ii) projections of λ from deterministic models would be higher than those of stochastic models,
(iii) projections of λ would be lowest for models with lagged effects, and
(iv) populations would be more skewed towards pre-reproductive size classes in fragments that forest, regardless of model structure

Methods

Study System and Demographic Data

Heliconia acuminata (Heliconiaceae) is a perennial, self-incompatible monocot that is distributed throughout much of the Amazon basin (Kress 1990). While some *Heliconia* species grow in large aggregations on roadsides, gaps, and in other disturbed habitats, others - including *H. acuminata* - grow primarily in the forest understory (Kress 1983; Ribeiro et al. 2010). Understory *Heliconia* species produce fewer flowers and are pollinated by traplining hummingbirds (Stouffer and Bierregaard 1996; Bruna et al. 2004). The models and analyses here are based on 11 years (1998-2009) of demographic data collected on >8500 *H. acuminata* found at Brazil's Biological Dynamics of Forest Fragments Project (BDFFP), located ~70 km north of Manaus, Brazil. The BDFFP reserves include both continuous forest and forest fragments that range in size from 1-100 ha. These fragment reserves were originally isolated in the early 1980's by the creation of cattle pastures, with the secondary growth surrounding them periodically cleared to ensure their continued isolation. The habitat in all sites is non-flooded lowland rain forest with rugged topography. A complete summary of the BDFFP and its history can be found in Bierregaard et al. (2001).

A complete description of the demographic methods, data, and analyses to date can be found in Bruna et al. (2023). Briefly, in 1997–1998 a series of 5000 m^2 plots were established in the BDFFP reserves: N=6 in Continuous Forest and N=4 in 1-ha Forest Fragments. All of the *Heliconia acuminata* in these plots were marked and measured; the plots were censused annually, at which time a team recorded the size of surviving individuals, marked and measured new seedlings, and identified any previously marked plants that died. Each

plot was also surveyed 4-5 times during the flowering season to identify reproductive plants; in our site *H. acuminata* begin flowering early in the rainy season (e.g., January) and most reproductive plants produce a single infloresence (range = 1–7) with 20–25 flowers (Bruna and Kress 2002). Fruits mature April-May and have 1–3 seeds per fruit ($\bar{x} = 2$) that are dispersed by a thrush and several species of manakin (Uriarte et al. 2011). Dispersed seeds germinate approximately 6 months after dispersal at the onset of the subsequent rainy season, with rates of germination and seedling establishment higher in continuous forest than forest fragments (Bruna 1999; Bruna and Kress 2002). On average olots in CF also had more than twice as many plants as the plots in 1-ha fragments (CF median = 788, range = (201-1549); 1-ha median = 339, range = (297-400)).

Construction of Integral Projection Models

We compared three classes of IPMs - Deterministic, Stochastic, and Stochastic with lagged effects of precipitation - each of which required different functional forms of their underlying vital rates models (Figure 1). All of the models were density-independent.

(1) Deterministic IPM: In this model, which served as the foundation for more complex models, the number and size of mature plants in year $t+1$ is determined by sub-kernels describing the survival and growth (or regression) of mature plants from year t to $t+1$, the number of seedlings establishing in year t that survive to $t+1$ (Equation 1), and the number of new seedlings that enter the population (Equation 2).

$$n(z', t+1) = R(z')n_s(t) + \int_L^U P(z', z)n(z, t)\, dz \tag{1}$$

$$n_s(t+1) = \int_L^U F(z)n(z, t)\, dz \tag{2}$$

In Equation 1 the sub-kernel $P(z', z)$ describes the size-dependent survival and growth or regression ($s(z)$ and $G(z', z)$, respectively) of mature plants from one year to the next (Equation 3). Sub-kernel $R(z')$ describes the survival and growth of seedlings that established in year t to year $t+1$ (Equation 4); note that these values are not size-dependent - in all our IPMs 'seedlings' are a discrete, size-independent category with a probability s_s of survival for one year following germination and establishment, with the size at which they transition into the 'mature' plant category given by $G(z', z)$. IPMs can include transitions between continuous and discrete states (Ellner et al. 2016)); we treat seedlings as a distinct category because they have lower survival and growth in their first year than comparably sized plants (Bruna 2003; Scott et al. 2022).

$$P(z', z) = s(z)G(z', z) \tag{3}$$

$$R(z') = s_s G_s(z') \tag{4}$$

The number of new seedlings entering the population, $n_s(t+1)$ (Equation 2), is described by the fecundity sub-kernel (Equation 5). Both the probability that a mature plant will

flower, $p_f(z)$, and the number of seeds they produce, $f(z)$, are size dependent. These seeds germinate and establish as seedlings with probability g.

$$F(z) = p_f(z)f(z)g \tag{5}$$

Vital rate models for growth ($G_s(z')$ and $G(z', z)$), survival (s_s and $s(z)$), and flowering ($p_f(z)$) were fit using the long-term demographic data (Bruna 2003). For established plants, these three vital rates were modeled as a smooth function of size in the previous census using generalized additive models (GAMs) fit with the `mgcv` package (Wood 2011) in R version 4.4.1 (2024-06-14) (R Core Team 2020). For consistency, seedling survival and growth were also modeled using GAMs, but without size in the previous census as a predictor (i.e. intercept only models). For growth models ($G_s(z')$ and $G(z', z)$) a scaled t family distribution provided a better fit to the data than a gaussian fit as the residuals were leptokurtic with a simple Gaussian model. Size-specific fecundity was based on surveys of fruits per flowering plant (Bruna 2021) and seeds per fruit (Bruna 2014) (together $f(z)$) and experimentally derived estimates of germination and establishment in forest and fragments (Bruna 1999, 2002) .

(2) Stochastic IPM: To build the stochastic, kernel-resampled IPMs we included environmental stochasticity in all vital rate models built using the long term demographic datset by adding a random effect of year (Figure 1). The random effect of year was included using a factor–smooth interaction which allowed the relationship between plant size and vital rates to vary in functional form among transition years. The kernel-resampling approach is to generate kernels corresponding to each transition year in the demographic dataset using the random smooths for year, and to iterate the IPM by drawing from these randomly. This is equivalent to the matrix selection approach for matrix population models described by Caswell (2001).

(3) Stochastic IPM with lagged effects of precipitation on vital rates: In our The stochastic, parameter-resampled IPMs the impacts of precipitation extremes on vital rates were modeled explicitly (*sensu* Metcalf et al. (2015)). We calculated the standardized precipitation evapotranspiraton index (SPEI) for our site using a published gridded dataset based on ground measurements (Xavier et al. 2016) as described in Scott et al. (2022). For all vital rate models fit using the long term demographic dataset, we modeled delayed effects of SPEI using distributed lag non-linear models with a maximum lag of 36 months (Scott et al. 2022) (Figure 1). To iterate these parameter-resampled IPMs, a random sequence of SPEI values was created by sampling years of the observed monthly SPEI data. Then, 36 month lags are calculated for each year starting in February (the month of the demographic census). These values are then used to predict fitted values from the vital rates models, generating different kernels at each iteration of the IPM. With this method, the kernels of successive iterations are not entirely independent because the SPEI values used in calculating vital rates include values used in the previous two iterations, but they are ergodic.

All IPMs were constructed and iterated using the `ipmr` package in R (Levin et al. 2021). The IPMs used 100 meshpoints and the midpoint rule for calculating kernels . For each

type of IPM we iterated the model for 1000 time steps, discarding the first 100 time steps to omit transient effects. Stochastic growth rates (λ_s) were calculated as the average $ln(\lambda)$ from each time step (Caswell 2001) and back-transformed to be on the same scale as deterministic lambdas for comparison. We used the distribution of established plant sizes and proportion of seedlings from the full dataset as a starting population vector. While other starting population vectors were possible, the choice is of little importance as it will only impact transient dynamics, which we aren't interested in for this study.

To estimate uncertainty around the per-capita growth rates (lambdas), we created 500 bootstraps of the demographic dataset by sampling individual plants with replacement within each habitat. For each bootstrap, we then re-fit vital rates models (all except germination and establishment rate, fruits per flowering plant, and seeds per fruit, which were estimated using different datasets), constructed IPMs, and calculated a value for lambda as described above. We then used these bootstraped estimates of lambda to calculate bias corrected 95% confidence intervals (Ellner et al. 2016).

#TODO: need to add something about the comparison of population structure (figure)
This workflow was managed using the `targets` R package (Landau 2021) which also allowed us to track computational time spent on each IPM for comparison.

Statistical analyses

Comparison of CF vs FF

- For det need to bootstrap
- for within stoch and lag: glm/t-test.

Results & Discussion

1. For all vital rates estimated using the long term demographic dataset, the DLNM model fit the best (dAIC = 0) followed by the model with a random effect of year, followed by the deterministic model (Table 1).

2. Population growth rates in CF were significantly higher than in forest fragments for all IPM types (Table 2).

3. Deterministic and stocuhastic-kernal similar means.
4. These results are consistent with those of Kaye and Pyke (2003), who found who found that the method effected stochastic lambda but relative ranking of populations was consistent.
5. BUT lag dropped lambdas considerably. In fact, took both well below zero. This is a big, big difference. If you are doing conservation and management, a growth rate lower by 5-6 % would really rock your world.

Population Structure

6. Figure 2 has some interesting things in it:
    - For the deterministic IPM (and the kernel-resampled IPM?) there are slightly more of the smallest plants and the largest plants in CF compared to FF (i.e. more medium sized plants in FF).
    - For the kernel-resampled IPM (random effect of year), the fluctuations are extremely similar between CF and FF
    - For the parameter-resampled IPM (DLNM) the size structure of the population is a LOT more variable in FF. This makes sense as we know lagged effects are more important in fragments.
    - Also, the fluctuations in size structure in CF do not match the fluctuations in FF as well (can see this by the increased spread of points in Figure 2 (B)
    - Also, in the parameter-resampled IPM (and only in this one), we see a shift toward smaller plants in FF compared to CF

Time and Effort

4. DLNM models take much, much longer to iterate: while the Deterministic and Kernel-resampled stochastic models took ~0.02 and ~0.07 min to iterate (respectively), the Parameter-resampled stochastic models with lagged effects took ~87.12 min.

5. The greater use of computational resources is likely a result of `predict()` being much slower for GAMs with 2D smooths because the number of knots is much higher compared to the GAMs used for the vital rates models in the determinsitic and kernel-resampled IPMs.

Acknowledgments

We thank , __, _____ and _____ anonymous reviewers for helpful discussions and comments on the manuscript. We thank Sam Levin for his help with the `ipmr` package. Financial support was provided by the U.S. National Science Foundation (awards _____, and _____). This article is publication no. – – in the BDFFP Technical series. The authors declare no conflicts of interest.

CRediT Statement

ERS contributed to the conceptualization, methodology, formal analysis, and led the writing of the original draft. EMB contributed to the conceptualization, methodology, and writing and also acquired funding.

Data Availability Statement

Data and R code used in this study are archived with Zenodo at *(doi and url to be added on acceptance)*.

Literature Cited

Beckerman, A., T. G. Benton, E. Ranta, V. Kaitala, and P. Lundberg. 2002. Population dynamic consequences of delayed life-history effects. Trends in Ecology & Evolution 17:263–269.

Bierregaard, R. O., C. Gascon, T. E. Lovejoy, and R. Mesquita, eds. 2001. Lessons from Amazonia: The ecology and conservation of a fragmented forest. Yale University Press, New Haven.

Brooks, M. E., K. Kristensen, M. R. Darrigo, P. Rubim, M. Uriarte, E. Bruna, and B. M. Bolker. 2019. Statistical modeling of patterns in annual reproductive rates. Ecology 100.

Bruna, E. M. 1999. Seed germination in rainforest fragments. Nature 402:139.

———. 2002. Effects of forest fragmentation on *Heliconia acuminata* seedling recruitment in central Amazonia. Oecologia 132:235–243.

Bruna, E. M. 2003. Are plant populations in fragmented habitats recruitment limited? Tests with an Amazonian herb. Ecology 84:932–947.

———. 2014. Dataset: <Span class="nocase">*Heliconia acuminata* seed set (seeds per fruit). Figshare doi: 10.6084/m9.figshare.1273926.v2.

———. 2021. Dataset: Leaf number, leaf area, shoot number, and height of reproductive H. acuminata. Zenodo https://doi.org/10.5281/zenodo.5041931.

Bruna, E. M., and W. J. Kress. 2002. Habitat fragmentation and the demographic structure of an Amazonian understory herb (*Heliconia acuminata*). Conservation Biology 16:1256–1266.

Bruna, E. M., W. J. Kress, F. Marques, and O. F. da Silva. 2004. *Heliconia acuminata* reproductive success is independent of local floral density. Acta Amazonica 34:467–471.

Bruna, E. M., O. Nardy, S. Y. Strauss, and S. Harrison. 2002. Experimental assessment of Heliconia acuminata growth in a fragmented Amazonian landscape. Journal of Ecology 90:639–649.

Bruna, E. M., and M. K. Oli. 2005. Demographic Effects of Habitat Fragmentation on a Tropical Herb: Life-Table Response Experiments. Ecology 86:1816–1824.

Bruna, E. M., M. Uriarte, M. R. Darrigo, P. Rubim, C. F. Jurinitz, E. R. Scott, O. Ferreira da Silva, et al. 2023. Demography of the understory herb Heliconia acuminata (Heliconiaceae) in an experimentally fragmented tropical landscape. Ecology 104:e4174.

Caswell, H. 2001. Matrix population models: Construction, analysis, and interpretation. Sinauer Associates, Sunderland.

Criley, R., and S. Lekawatana. 1994. Year around production with high yields may be a possibility for *Heliconia chartacea*. Acta Horticulturae, New ornamental crops and the market for floricultural products 397:95–102.

Crone, E. E., E. S. Menges, M. M. Ellis, T. Bell, P. Bierzychudek, J. Ehrlen, T. N. Kaye, et al. 2011. How do plant ecologists use matrix population models? Ecology Letters 14:1–8.

Ellner, S. P., D. Z. Childs, and M. Rees. 2016. Data-driven modelling of structured populations: A practical guide to the integral projection model. Springer Science+Business Media, New York, NY.

Ellner, S. P., and M. Rees. 2006. Integral projection models for species with complex demography. American Naturalist 167:410–428.

Evers, S. M., T. M. Knight, D. W. Inouye, T. E. X. Miller, R. Salguero-Gómez, A. M. Iler, and A. Compagnoni. 2021. Lagged and dormant season climate better predict plant vital rates than climate during the growing season. Global Change Biology 27:1927–1941.

Kaye, T. N., and D. A. Pyke. 2003. The effect of stochastic technique on estimates of population viability from transition matrix models. Ecology 84:1464–1476.

Kress, J. 1990. The diversity and distribution of *heliconia* (Heliconiaceae) in Brazil. Acta Botanica Brasileira 4:159–167.

Kress, W. J. 1983. Self-incompatibility systems in Central American *heliconia*. Evolution 37:735–744.

Kuss, P., M. Rees, H. H. Ægisdóttir, S. P. Ellner, and J. Stöcklin. 2008. Evolutionary demography of long-lived monocarpic perennials: A time-lagged integral projection model. Journal of Ecology 96:821–832.

Landau, W. M. 2021. The targets R package: A dynamic Make-like function-oriented pipeline toolkit for reproducibility and high-performance computing 6:2959.

Levin, S. C., D. Z. Childs, A. Compagnoni, S. Evers, T. M. Knight, and R. Salguero-Gómez. 2021. Ipmr: Flexible implementation of Integral Projection Models in R. Methods in Ecology and Evolution 12:1826–1834.

Metcalf, C. J. E., S. P. Ellner, D. Z. Childs, R. Salguero-Gómez, C. Merow, S. M. McMahon, E. Jongejans, et al. 2015. Statistical modelling of annual variation for inference on stochastic population dynamics using Integral Projection Models. Methods in Ecology and Evolution 6:1007–1017.

Molowny-Horas, R., M. L. Suarez, and F. Lloret. 2017. Changes in the natural dynamics of *Nothofagus dombeyi* forests: Population modeling with increasing drought frequencies. Ecosphere 8:1–17.

Morris, W. F., and D. F. Doak. 2002. Quantitative conservation biology: Theory and practice of population viability analysis. Sinauer, Sunderland, MA.

R Core Team. 2020. *R: A language and environment for statistical computing*. Vienna, Austria.

Rees, M., D. Z. Childs, and S. P. Ellner. 2014. Building integral projection models: A user's guide. Journal of Animal Ecology 83:528–545.

Rees, M., and S. P. Ellner. 2009. Integral projection models for populations in temporally varying environments. Ecological Monographs 79:575–594.

———. 2016. Evolving integral projection models: Evolutionary demography meets eco-evolutionary dynamics. Methods in Ecology and Evolution 7:157–170.

Ribeiro, M. B. N., E. M. Bruna, and W. Mantovani. 2010. Influence of post-clearing treatment on the recovery of herbaceous plant communities in Amazonian secondary forests. Restoration Ecology 18:50–58.

Salguero-Gómez, R., O. R. Jones, C. R. Archer, Y. M. Buckley, J. Che-Castaldo, H. Caswell, D. Hodgson, et al. 2015. The COMPADRE Plant Matrix Database: An open online repository for plant demography. (M. Rees, ed.)Journal of Ecology 103:202–218.

Scott, E. R., M. Uriarte, and E. M. Bruna. 2022. Delayed effects of climate on vital rates lead to demographic divergence in Amazonian forest fragments. Global Change Biology 28:463–479.

Stouffer, P. C., and R. O. Bierregaard. 1996. Forest fragmentation and seasonal patterns of hummingbird abundance in Amazonian Brazil. Ararajuba 4:9–14.

Tenhumberg, B., E. E. Crone, S. Ramula, and A. J. Tyre. 2018. Time-lagged effects of weather on plant demography: Drought and *Astragalus scaphoides*. Ecology 99:915–925.

Tuljapurkar, S. 1990. Population Dynamics in Variable Environments. (S. Levin, ed.)Lecture Notes in Biomathematics (Vol. 85). Springer, Berlin, Heidelberg.

Uriarte, M., M. Anciães, M. T. B. da Silva, R. Rubim, E. Johnson, and E. M. Bruna. 2011. Disentangling the drivers of reduced long-distance seed dispersal by birds in an experimentally fragmented landscape. Ecology 92:924–937.

Williams, J. L., H. Jacquemyn, B. M. Ochocki, R. Brys, T. E. X. Miller, and R. Sheffer-

351 son. 2015. Life history evolution under climate change and its influence on the population
352 dynamics of a long-lived plant. Journal of Ecology 103:798–808.

353 Williams, J. L., T. E. Miller, and S. P. Ellner. 2012. Avoiding unintentional eviction from
354 integral projection models. Ecology 93:2008–2014.

355 Wood, S. N. 2011. Fast stable restricted maximum likelihood and marginal likelihood esti-
356 mation of semiparametric generalized linear models 73:3–36.

357 Xavier, A. C., C. W. King, and B. R. Scanlon. 2016. Daily gridded meteorological variables
358 in Brazil (1980–2013). International Journal of Climatology 36:2644–2659.

Table 1: Comparison of vital rate models used to build IPM. The 'Effect of Environment' column describes how environmental effects were included in models. Those with 'none' were used to build deterministic IPMs; those with a random effect of year were used to build stochastic, kernel-resampled IPMs; and those with a distributed lag non-linear model (DLNM) were used to build stochastic, parameter-resampled IPMs. 'edf' is the estimated degrees of freedom of the penalized GAM. ΔAIC is calculated within each habitat and vital rate combination. ΔAIC within 2 indicates models are equivalent.

Habitat	Vital Rate	Effect of Environment	edf	ΔAIC
CF	Survival	Random effect of year	43.26	0
CF	Survival	DLNM	19.72	78.92
CF	Survival	None	4.976	260
CF	Growth	Random effect of year	78.43	0
CF	Growth	DLNM	23.87	158.5
CF	Growth	None	7.81	1896
CF	Flowering	DLNM	19.59	0
CF	Flowering	Random effect of year	17.19	1.627
CF	Flowering	None	7.468	381.9
CF	Seedling survival	None	1	0
CF	Seedling survival	Random effect of year	1.817	1.386
CF	Seedling survival	DLNM	4.008	1.528
CF	Seedling growth	Random effect of year	9.475	0
CF	Seedling growth	DLNM	8.952	2.902
CF	Seedling growth	None	1	172.3
FF	Survival	DLNM	14.95	0
FF	Survival	Random effect of year	19.21	35.68
FF	Survival	None	4.333	51.25
FF	Growth	DLNM	25.18	0
FF	Growth	Random effect of year	37.84	200
FF	Growth	None	5.599	382.8
FF	Flowering	DLNM	20.61	0
FF	Flowering	Random effect of year	13.81	27.4
FF	Flowering	None	5.007	101.7
FF	Seedling survival	DLNM	5.574	0
FF	Seedling survival	Random effect of year	5.088	5.721
FF	Seedling survival	None	1	6.491
FF	Seedling growth	Random effect of year	6.25	0
FF	Seedling growth	DLNM	8.182	2.29
FF	Seedling growth	None	1	5.745

Table 2: Population growth rates for continuous forest (CF) and forest fragments (FF) under different kinds of IPMs with bootstrapped, bias-corrected, 95% confidence intervals.

IPM	Habitat	λ
Deterministic	FF	0.9778 (0.9736, 0.9823)
Deterministic	CF	0.9897 (0.9877, 0.9920)
Stochastic, kernel-resampled	FF	0.9787 (0.9735, 0.9835)
Stochastic, kernel-resampled	CF	0.9913 (0.9892, 0.9939)
dlnm	FF	0.9595 (0.9459, 0.9689)
dlnm	CF	0.9795 (0.9752, 0.9867)

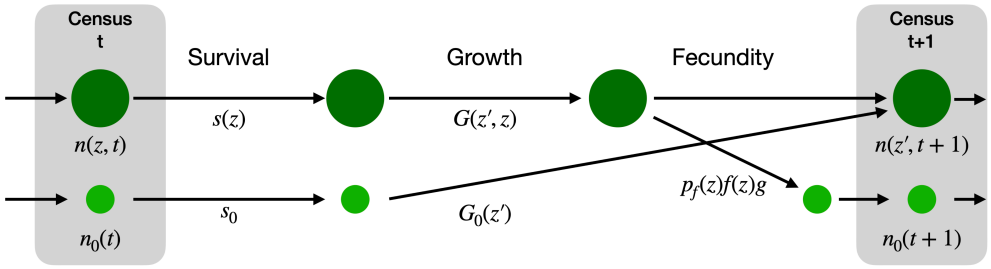

Description	Deterministic	Stochastic, kernel-resampled	Stochastic, parameter-resampled
Survival	$s(z)$	$s_y(z)$	$s(z;\theta_{0-36})$
Growth	$G(z';z)$	$G_y(z';z)$	$G(z',z;\theta_{0-36})$
Flowering	$p_f(z)$	$p_{f_y}(z)$	$p_f(z;\theta_{0-36})$
Size-specific fecundity	$f(z)$	$f(z)$	$f(z)$
Germination & establishment	g	g	g
Seedling survival	s_0	s_{0_y}	$s_0(\theta_{0-36})$
Seedling growth	$G_0(z')$	$G_{0_y}(z')$	$G_0(z';\theta_{0-36})$

Figure 1: Lifecycle diagram of *Heliconia acuminata*. Each transition is associated with an equation for a vital rate function. The functions shown on the diagram correspond to those used to construct a general, density-independent, deterministic IPM. The table below shows the equivalent equations for stochastic, kernel-resampled IPMs and stochastic, parameter-resampled IPMs.

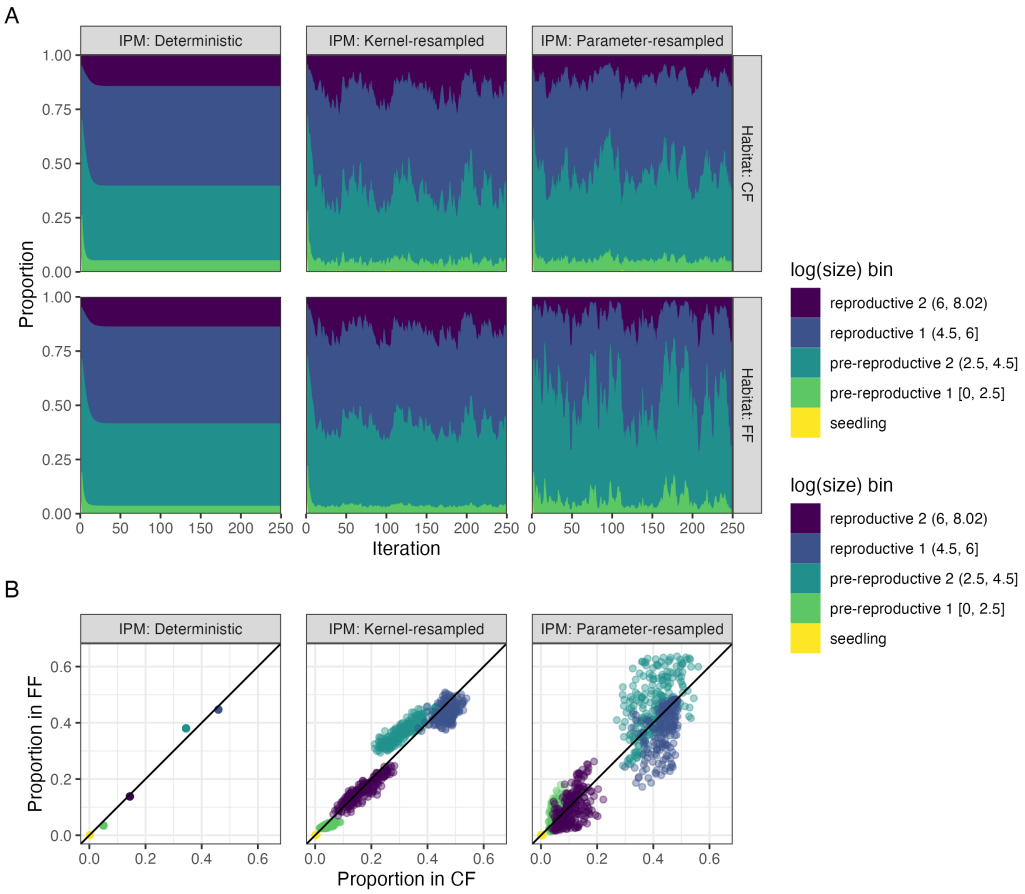
A
IPM: Deterministic
IPM: Kernel-resampled
IPM: Parameter-resampled
Habitat: CF
Habitat: FF
Proportion
1.00
0.75
0.50
0.25
0.00
0
50
100
150
200
250
Iteration
log(size) bin
reproductive 2 (6, 8.02)
reproductive 1 (4.5, 6]
pre-reproductive 2 (2.5, 4.5]
pre-reproductive 1 [0, 2.5]
seedling
B
Proportion in FF
Proportion in CF
0.0
0.2
0.4
0.6

Figure 2